Molecular Biology of the Cell
Vol. 11, 2949–2959, September 2000

Bim1p/Yeb1p Mediates the Kar9p-dependent Cortical Attachment of Cytoplasmic Microtubules

Rita K. Miller,* Soo-Chen Cheng,† and Mark D. Rose‡

Department of Molecular Biology, Lewis Thomas Laboratory, Princeton University, Princeton, New Jersey 08544

Submitted February 22, 2000; Revised June 23, 2000; Accepted July 5, 2000
Monitoring Editor: Douglas Koshland

In *Saccharomyces cerevisiae*, positioning of the mitotic spindle depends on the interaction of cytoplasmic microtubules with the cell cortex. In this process, cortical Kar9p in the bud acts as a link between the actin and microtubule cytoskeletons. To identify Kar9p-interacting proteins, a two-hybrid screen was conducted with the use of full-length Kar9p as bait, and three genes were identified: *BIM1*, *STU2*, and *KAR9* itself. *STU2* encodes a component of the spindle pole body. Bim1p is the yeast homologue of the human microtubule-binding protein EB1, which is a binding partner to the adenomatous polyposis coli protein involved in colon cancer. Eighty-nine amino acids within the third quarter of Bim1p was sufficient to confer interaction with Kar9p. The two-hybrid interactions were confirmed with the use of coimmunoprecipitation experiments. Genetic analysis placed Bim1p in the Kar9p pathway for nuclear migration. Bim1p was not required for Kar9p's cortical or spindle pole body localization. However, deletion of *BIM1* eliminated Kar9p localization along cytoplasmic microtubules. Furthermore, in the *bim1* mutants, the cytoplasmic microtubules no longer intersected the cortical dot of Green Fluorescent Protein–Kar9p. These experiments demonstrate that the interaction of cytoplasmic microtubules with the Kar9p cortical attachment site requires the microtubule-binding protein Bim1p.

INTRODUCTION

In the budding yeast *Saccharomyces cerevisiae*, the plane of cytokinesis is established by the position of the emerging bud. Therefore, to ensure that both the mother and daughter cell receive a nucleus upon completion of cytokinesis, the spindle must migrate to the mother–bud neck and become correctly oriented along the long axis of the dividing cell before cytokinesis. Cytoplasmic microtubules play a central role in nuclear positioning (Palmer *et al.*, 1992; Sullivan and Huffaker, 1992). The cytoplasmic microtubules are attached at their minus ends to a centrosome-like structure embedded within the nuclear envelope termed the spindle pole body (SPB) (Byers, 1981). At their plus ends, the cytoplasmic microtubules exhibit dynamic instability (Shaw *et al.*, 1997) while searching for their cortical attachment site (Carminati and Stearns, 1997). Microtubule interactions with the cortex have been observed to be coordinated with movements of the nucleus toward the bud (Carminati and Stearns, 1997). Microtubule cortical attachment is mediated by actin, Kar9p, Bud6p, and Bni1p (Lee *et al.*, 1999; Miller *et al.*, 1999), and microtubules are seen to intersect with a cortical dot of Kar9p (Miller and Rose, 1998). Kar9p's localization as a single dot at the tip of the bud is dependent on actin (Miller *et al.*, 1999), consistent with actin's role in spindle positioning (Palmer *et al.*, 1992; Theesfeld *et al.*, 1999).

Several proteins are thought to act on the cytoplasmic microtubules during nuclear migration, altering parameters such as microtubule length, dynamics, and/or force production. Among these are dynein and components of the dynactin complex (Clark and Meyer, 1994; McMillan and Tatchell, 1994; Muhua *et al.*, 1994; Carminati and Stearns, 1997; Kahana *et al.*, 1998). Dynein is thought to provide part of the force for nuclear migration, and mutations in dynein result in mitosis occurring within the mother cell and reduce the dynamic nature of the cytoplasmic microtubules (Yeh *et al.*, 1995; Carminati and Stearns, 1997). Several kinesins, Kip2p, Kip3p, and Kar3p, have also been implicated in nuclear migration (Cottingham and Hoyt, 1997; DeZwaan *et al.*, 1997; Saunders *et al.*, 1997; Miller *et al.*, 1998). In addition, Num1p, a cortical protein in the mother cell (Farkasovsky and Kuntzel, 1995), and Bik1p, a MAP required for microtubule stability and function (Trueheart *et al.*, 1987; Berlin *et al.*, 1990), play significant roles in nuclear migration.

* Present address: Department of Biology, University of Rochester, Rochester, NY 14627.
† Permanent address: Institute of Molecular Biology, Academia Sinica, Nankang, Taiwan.
‡ Corresponding author. E-mail address: mrose@molbio.princeton.edu.
Abbreviations used: APC, adenomatous polyposis coli; GFP, Green Fluorescent Protein; HA, hemagglutinin; SC, synthetic complete; SPB, spindle pole body.

Table 1. Yeast strains used in this study

Strain	Genotype	Source
MS1556	*MAT***a** *ura3-52 leu2-3 leu2-112 ade2-101 his3Δ-200*	Rose
MS4263	*MAT***a** *kar9Δ::LEU2 ura3-52 leu2-3 leu2-112 ade2-101 his3Δ-200*	Rose
MS4306	*MAT***a** *kar9Δ::HIS3 ura3-52 leu2-3 leu2-112 ade2-101 his3Δ-200*	Rose
MS4315	*MATα kar9Δ::LEU2 ura3-52 leu2-3 leu2-112*	This study
MS4998	*MATα dhc1Δ::URA3 ura3-52 leu2-3 leu2-112 ade2-101 his3Δ-200*	This study
MS7310	*MAT***a** *BIM1::KAN ura3-52 leu2-3 leu2-112 ade2-101 his3Δ-200*	This study
MY7309	*MAT***a** *BIM1::KAN trp1-901 leu2-3 leu2-112 ura3-52 his3-200 gal4Δ gal80Δ LYS2::GAL1-HIS3 GAL2-ADE2met3::GAL7-lacZ*	This study
PJ69-4A	*MAT***a** *trp1-901 leu2-3 leu2-112 ura3-52 his3-200 gal4Δ gal80Δ LYS2::GAL1-HIS3 GAL2-ADE2 met3::GAL7-lacZ*	James *et al.* (1996)

Bim1p is the yeast homologue of human EB1, a protein that binds at the carboxyl terminus of the adenomatous polyposis coli (APC) tumor-suppressor protein (Su *et al.*, 1995). APC is a multifunctional protein involved in the Wnt signaling pathways of higher eukaryotic pattern formation (Barth *et al.*, 1997; Barker *et al.*, 2000), and mutations in APC are the cause of human colorectal cancers (Groden *et al.*, 1991). In yeast, Bim1p has been shown to regulate microtubule dynamics, exerting its greatest effect during G1 (Tirnauer *et al.*, 1999). Mutations in *BIM1* and dynactin components are synthetically lethal with each other, suggesting that they act in different and partially redundant pathways (Muhua *et al.*, 1998). Bim1p has also been implicated in the cytokinesis delay found in dynein mutants (Muhua *et al.*, 1998). In both yeast and humans, EB1 binds along the microtubule network, with increased concentration at the distal tips (Schwartz *et al.*, 1997; Berrueta *et al.*, 1998; Morrison *et al.*, 1998; Tirnauer *et al.*, 1999).

To better understand the mechanism of Kar9p's microtubule-orientation function, we carried out a two-hybrid screen with the use of Kar9p as bait and identified Bim1p, Stu2p, and Kar9p as Kar9p-interacting proteins. These interactions were confirmed by coimmunoprecipitation experiments. Genetic analysis placed Bim1p in the Kar9p pathway for nuclear migration. Deletion of *BIM1* did not alter Kar9p's localization as a single dot at the tip of the bud or its localization near the SPB. However, Bim1p was required for the localization of Kar9p along cytoplasmic microtubules. Whereas in wild-type cells microtubules usually intersected the single cortical dot of Green Fluorescent Protein (GFP)–Kar9p, in *bim1* mutants the microtubules only rarely intersected cortical GFP–Kar9p. These experiments indicate that the interaction of cytoplasmic microtubules with the Kar9p cortical attachment site requires the microtubule-binding protein Bim1p.

MATERIALS AND METHODS

Cell Culture and Fixation Methods

Yeast strains and plasmids used in this study are listed in Tables 1 and 2. Cells were grown in yeast peptone dextrose or in synthetic complete (SC) media as described previously (Miller and Rose, 1998). For experiments localizing GFP–Kar9p, strains containing the plasmid pMR3465 were grown, induced with 2% galactose, and fixed with formaldehyde as described previously (Miller and Rose, 1998).

Two-Hybrid Screen

A two-hybrid screen was used to identify Kar9p-interacting proteins. A full-length *KAR9* fragment engineered with terminal *Sal*I restriction sites was synthesized by PCR. This was fused in-frame to the DNA-binding domain of *GAL4* at the *Sal*I site of pGBDU-C3 (James *et al.*, 1996) to create the plasmid pMR4150. The three genomic libraries were transformed independently into the reporter strain PJ69-4A (James *et al.*, 1996) containing pMR4150 by the method of Gietz and Schiestl (1995). This reporter strain contains three different reporter genes, each driven by a different GAL promoter, reducing the probability of false positives. Transformants were selected at 30°C on SC plates lacking uracil and leucine. To test for activation of the *GAL2–ADE2* indicator, $\sim 6 \times 10^6$ transformants were replica printed to SC plates lacking uracil, leucine, and adenine and grown at 30°C. Ade^+ transformants were recovered at a frequency of 1:37,500. After recovery of the prey plasmids from yeast and amplification in *Escherichia coli* (Hoffman and Winston, 1987), plasmids that retested positive for activation of both the *GAL1–HIS3* and *GAL7–lacZ* reporters were identified. β-Galactosidase activity was assayed in crude extracts as described previously (Rose *et al.*, 1990). In control experiments, the plasmids failed to activate the reporters in strains lacking a DNA-binding domain plasmid, strains containing an empty DNA-binding domain plasmid, and strains containing irrelevant bait fused to the DNA-binding domain of Gal4p, indicating a specific interaction. A combination of Southern blotting and sequencing was used to identify the fusion clones.

Strain Construction

Isogenic deletion mutants were constructed in the wild-type strain MS1556, which was derived from S288C. To construct *bim1*Δ::*KAN*, all but the first codon of *BIM1* was replaced with *KAN* with the use of the one-step gene-replacement method (Rothstein, 1983). The

Table 2. Plasmids used in this study

Plasmid	Description/markers	Source
pMR4150	GAL4 DNA-binding domain-*KAR9, URA3*, Amp^R, 2μ	This study
pMR4620	P_{GAL1}-*BIM1*-V5-his_6 Amp^R *URA3* 2μ	Invitrogen
pMR3143	*KAR9* CEN *HIS3*	This study
pMR4721	*KAR9::HA* CEN *HIS3*	This study
pMR4722	*KAR9* 2μ *HIS3*	This study
pMR4723	*KAR9::HA* 2μ *HIS3*	This study
pWP70	*STU2*::HA_3 *LEU2* Amp^R CEN	T. Huffaker

disruption fragment was generated by PCR with the use of the following two oligonucleotides (Life Technologies, Grand Island, NY) (the *BIM1* sequence is shown in normal font and the *KAN* sequence is shown in bold italics): 5′GAA ACA AGT CAA AAA AAA TTG AAG GCA GAC TCA AAA GCA AGG ATA ATA TTC CAC CAA ATC AGG GAC GAA GCA ATG ***GAT ATC AAG CTT GCC TCG TC*** 3′ and 5′ATT GAT AC GAG TAA TAA AAA AAA TAA AAA AAA ATA ATA CAT ATT CGA AAA CAA TAC TGC TTT TTA GTT CTC AAC TTA ***GTC GAC ACT GGA TGG CGG***3′. The plasmid pFA-MX2 (Wach *et al.*, 1994) was used as the template for the *KAN* portion of the disruption construct. The wild-type strain MS1556 and the two-hybrid reporter strain PJ69-4A were transformed and selected for *KAN* prototrophy on yeast peptone dextrose plates containing 150 μg/ml geneticin (Sigma Chemical, St. Louis, MO) to create MS7310 and MY7309. Replacement of *BIM1* was confirmed by PCR and Southern blot analysis.

For immunoprecipitation experiments, a triple hemagglutinin (HA) epitope–tagged form of Kar9p was created. A fragment coding for a triple HA tag with *Bgl*II ends was synthesized by PCR with the use of the GTEPI plasmid (from Bruce Futcher, Cold Spring Harbor Laboratory, Cold Spring Harbor, NY) as a template. The following primers were used: 5′GAC AAG ATC TCT TAC CCA TAC GAT GTT3′ and 5′CGG AGA TCT TAG CGT AAT CTG GGA C3′. The *KAR9*-containing CEN plasmid, pMR3143, was cut with *Bam*HI, and the HA-containing insert was ligated into it to produce the plasmid pMR4721. The *KAR9*-containing *Apa*I–*Sac*I fragment was excised from pMR4721 and ligated into the 2μ plasmid pRS423 (Sikorski and Hieter, 1989) to create pMR4723. To create an equivalent untagged control plasmid, the *KAR9*-containing *Apa*I–*Sac*I fragment of pMR3143 was ligated into pRS423 to create pMR4722.

Preparation of Kar9p Antibodies

A Kar9p::his6x plasmid (pMR3414) was created by cloning a *Bgl*II–*Dra*III fragment of *KAR9* lacking the first six codons into the *Bam*HI–*Sal*I sites of the pET-30(+) bacterial expression vector (Novagen, Madison, WI). The Kar9p::his6x fusion protein was purified from a 5-l culture of BL21(DE3) induced with 1 mM isopropylthio-β-galactoside for 6 h at 23°C. Cells were lysed by sonication in 8 M urea, 5 mM imidazole, 500 mM NaCl, and 20 mM Tris-HCl, pH 7.2, with protease inhibitors. The Kar9p fusion protein was purified by nickel-affinity chromatography with the use of a 100–300 mM elution gradient of imidazole in the same buffer. Fractions were pooled and dialyzed into PBS. Antibodies were produced in female New Zealand White rabbits at the Princeton University Animal Facility (Princeton, NJ).

Immunoprecipitations

Strains containing *BIM1*::V5 (Invitrogen, Carlsbad CA) and/or *KAR9* plasmids were grown to mid exponential phase in SC medium minus histidine and uracil. Bim1p::V5 expression was induced by the addition of 2% galactose for 4 h. Cells were washed once with ice-cold buffer B150 (50 mM Tris, pH 7.4, 150 mM NaCl, 0.2% Triton X-100 with protease inhibitors), resuspended in cold buffer B150 with protease inhibitors, and broken open by vortexing with glass beads. Crude cell lysates were transferred to a new microcentrifuge tube and centrifuged for 30 min at 14,000 × *g*. The supernatant was removed and recentrifuged for 10 min at 14,000 × *g*. V5 and HA antibodies were conjugated to beads as follows. HA antibody [clone HA.11(16B12), BAbCo, Richmond, CA] was coupled to cyanogen bromide–activated agarose beads (Amersham Pharmacia Biotech, Piscataway, NJ) according to the manufacturer's instructions with the use of 1.5 μg of antibody per 1 μl of resin. V5 antibody (Invitrogen) was coupled to protein A–Sepharose beads (Amersham Pharmacia Biotech) as described by Harlow and Lane (1988) with the use of 2 μg of V5 antibody per 1 μl of resin. For α-HA immunoprecipitations, 30 μl of conjugated resin was used. For α-V5 immunoprecipitations, 10 μl of resin was used for each reaction. For both V5 and HA immunoprecipitations, conjugated beads were added to 1.1 mg of total cellular protein and incubated for 1–2 h at 4°C and washed four times with 1 ml of buffer B150. Proteins were eluted with 2% SDS (50 μl for α-HA and 25 μl for α-V5) for 30 min at 4°C. Laemmli sample buffer (3×) was added to 0.5 volume, and samples were boiled for 5 min. Ten microliters of each sample was run on 10% SDS-PAGE for Western blotting.

For Stu2p–Kar9p coimmunoprecipitations, cells were grown to mid exponential phase in SC medium minus histidine. Cells were washed once in P250 buffer (PBS plus 100 mM NaCl and 0.2% Tween-20). Cells were resuspended in P250 buffer with protease inhibitors and broken open with glass beads. Crude cell lysates were transferred to a new microcentrifuge tube and centrifuged for 30 min at 14,000 × *g*. The supernatant was clarified a second time for 10 min at 14,000 × *g*. Three microliters of α-HA (12CA5) was added to 1.5 mg of extract and incubated overnight at 4°C. Extracts were centrifuged for 15 min at 14,000 × *g*. The supernatants were transferred to a new microfuge tube and reclarified for 10 min at 14,000 × *g*. Extracts were incubated with 15 μl of 50% protein A–conjugated Sepharose beads (Amersham Pharmacia Biotech) for 2 h at 4°C. Beads were washed six times in P250 buffer and resuspended in 30 μl of sample buffer. Samples were electrophoretically separated by 10% SDS-PAGE and transferred to nitrocellulose.

For Kar9p–Kar9p immunoprecipitations, cells were grown to mid exponential phase in SC medium minus leucine and histidine. GFP–Kar9p expression was induced by the addition of 2% galactose for 4 h. Extracts were prepared and immunoprecipitations were carried out as described above for Stu2p immunoprecipitations, except that buffer B150 with protease inhibitors was used for all washes. Two microliters of rabbit α-GFP (a kind gift from Jason Kahana and Pamela Silver, Dana Farber Cancer Institute, Boston, MA) was incubated with 1 mg of extract overnight at 4°C.

Microscopy

Indirect immunofluorescence was carried out as described previously (Miller and Rose, 1998). Microscopy was carried out with the use of an Axiophot microscope equipped with a 1.3 numerical aperture 100X FLUAR lens (Carl Zeiss, Thornwood, NY) or a 1.3 numerical aperture 100X UplanFl iris lens (Olympus, Tokyo, Japan). Images were recorded with the use of a Hamamatsu SIT Video Camera 3200 (Hamamatsu, Hamamatsu City, Japan) with a Hamamatsu camera controller C2400. Images were initially processed with the use of an Omnex image-processing unit (Imagen, Princeton, NJ) and captured to computer disk with the use of a Scion image-capture board (Las Vegas, NV). Adobe (Mountain View, CA) Photoshop 4.0 was used to optimize contrast in printed images.

RESULTS

A Two-Hybrid Screen Identified Bim1p, Stu2p, and Kar9p as Kar9p-interacting Proteins

Kar9p is required for cytoplasmic microtubule orientation during nuclear migration in *S. cerevisiae*, and the microtubules are observed to intersect a dot of Kar9p at the cell cortex during migration (Miller and Rose, 1998; Miller *et al.*, 1999). To better understand the mechanism of Kar9p-based microtubule attachment to the cortex, we sought to identify proteins that interact with Kar9p. A two-hybrid screen (James *et al.*, 1996) was carried out with the use of full-length Kar9p fused to the Gal4 DNA-binding domain as bait (see MATERIALS AND METHODS). Retrieval and sequencing of the strongest positive-interacting library plasmids identified clones containing the *STU2*, *KAR9*, and *BIM1* genes (Figure 1).

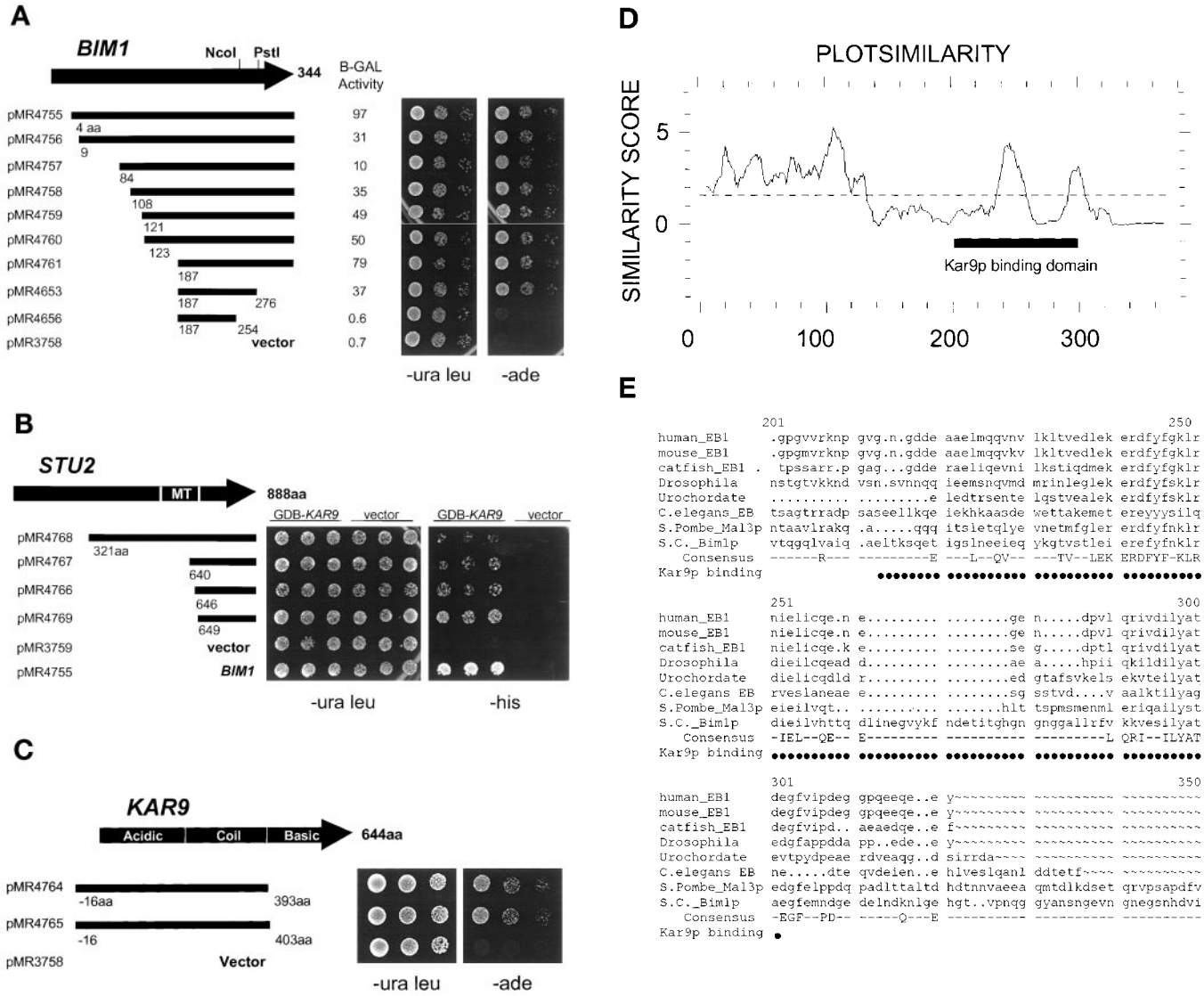

Figure 1. Kar9p interacts with Bim1p, Stu2p, and Kar9p by two-hybrid analysis. (A) The wild-type two-hybrid strain (PJ69-4A) containing pGDB-*KAR9* (pMR4150) and the indicated pGAD-*BIM1* library-positive plasmids were serially diluted 10-fold and spotted onto plates lacking uracil and leucine (−ura leu) or adenine (−ade). Plates were photographed after 2 d at 30°C. (B) A two-hybrid reporter strain deleted for *BIM1* (MY7309) containing either GDB-*KAR9* (pMR4150) or empty GDB vector (pMR3763) was transformed with the indicated *STU2* plasmids and assayed for activation of the *HIS3* reporter gene. The microtubule-binding domain of Stu2p (MT) has been mapped to amino acids 558–658 (Wang and Huffaker, 1997). Three independent *STU2* transformants are shown. Plates were photographed after 3 d at 30°C. (C) The wild-type two-hybrid strain (PJ69-4A) containing pGDB-*KAR9* (pMR4150) and the indicated *KAR9* library plasmids were serially diluted 10-fold and spotted onto plates lacking uracil and leucine (−ura leu) or adenine (−ade). Plates were photographed after 2 d at 30°C. (D and E) The Genetics Computer Group (Madison, WI) programs Plotsimilarity and Pretty were used to compare the EB1 homologues from human (accession number I52726), mouse (accession number AAA96320), catfish (accession number AAD31035), *D. melanogaster* (accession number AAD27859), urochordate (accession number CAA67697), *C. elegans* (accession number CAA20332), *S. pombe* (accession number Q10113), and *S. cerevisiae* (accession number NP 010932). (E) The BLOSUM62 amino acid substitution matrix was used for calculations. Additional parameters were set as GapLengthWeight, 2; GapWeight, 8. A consensus was noted if six or more residues were similar. The location of the Kar9p-binding domain is indicated by closed circles.

Bim1p is a 344-amino acid microtubule-associated protein involved in regulating cytoplasmic microtubule dynamics (Schwartz *et al.*, 1997; Tirnauer *et al.*, 1999). We isolated seven independent *BIM1* fusions in the screen that form a series of nested amino-terminal truncations. The largest deletion removed the 186 amino-terminal amino acids of Bim1p (Figure 1). To determine the minimal region of Bim1p required for interaction with Kar9p, two additional carboxyl-terminal truncations were generated with the use of unique *Nco*I and *Pst*I restriction sites in the *BIM1* gene

(Figure 1). The *Pst*I deletion removed 68 amino acids from the carboxyl terminus. This plasmid still interacted with Kar9p, as indicated by positive *GAL7–lacZ* and *GAL2–ADE2* reporter assays (Figure 1). However, the *Nco*I site deletion, which removed an additional 22 amino acids, eliminated interaction between the Kar9p and Bim1p fusion proteins (Figure 1). These data indicate that an 89-amino acid segment located at positions 187–276 within Bim1p is sufficient to confer interaction with Kar9p.

This segment includes a region that is highly conserved between the human, mouse, catfish, *Drosophila melanogaster*, urochordate, *Caenorhabditis elegans*, and *Schizosaccharomyces pombe* homologues of Bim1p (Figure 1, D and E). Interestingly, a stretch of ~20 amino acids at positions 233–253 is extremely conserved between the eight homologues. If the function of Kar9p is conserved, these residues in EB1/Bim1p are likely to be important for binding a Kar9p-like protein in higher eukaryotes.

The two-hybrid screen also identified four different clones of *STU2* (Figure 1B) that activated all three reporter genes. *STU2* encodes an 888-amino acid component of the SPB (Wang and Huffaker, 1997). The smallest *STU2* clone obtained from the library encodes residues 649–888 of Stu2p, a region adjacent to the microtubule-binding domain of Stu2p (Figure 1B). Stu2p has also been shown to interact with Bim1p by two-hybrid analysis (Chen *et al.*, 1998). To determine whether the Kar9p–Stu2p interaction might occur by a tertiary interaction including Bim1p, we deleted the *BIM1* gene from the two-hybrid reporter strain PJ69-4A. Although activation of the more stringent *ADE2* reporter was no longer observed (our unpublished results), all of the *STU2* fusions activated the *HIS3* reporter gene in strains containing the *KAR9* bait but not empty vector (Figure 1B). Interestingly, the shortest *STU2* fusion (pMR4769), which lacked the microtubule-binding domain, activated more strongly than the largest *STU2* fusion (pMR4768), which contained the microtubule-binding domain. We conclude that Kar9p interacts with Stu2p independent of both Bim1p and microtubules, although Bim1p may promote the Kar9p–Stu2p interaction.

Three independent clones of *KAR9* were also identified in the screen. For each, the *KAR9–GAL4* fusion junction was 16 codons upstream of, but in frame with, Kar9p's predicted methionine start site (Figure 1C). In these plasmids, *KAR9* was truncated at codons 393 and 403 (Figure 1C) and the Kar9p hybrid proteins would lack the highly basic carboxyl-terminal domain (calculated isoelectric point > 11.4; Miller and Rose, 1998). Thus, it is likely that Kar9p can self-oligomerize and that the basic domain is not required for this interaction. The central region of Kar9p includes two regions predicted to form coiled coils (Miller and Rose, 1998) that may be important for this interaction.

Coimmunoprecipitations Demonstrate that Bim1p, Stu2p, and Kar9p Physically Interact with Kar9p

Both Bim1p and Stu2p bind microtubules (Schwartz *et al.*, 1997; Wang and Huffaker, 1997), and Bim1p has been reported to be involved in nuclear positioning (Schwartz *et al.*, 1997; Tirnauer *et al.*, 1999). Therefore, we further investigated the interaction of these proteins with Kar9p. To confirm the two-hybrid data, we first tested whether Kar9p could coimmunoprecipitate with Bim1p and vice versa. To aid the analysis, we created a plasmid containing a functional Kar9p tagged with a triple-HA epitope. The tagged *KAR9* fully complemented the nuclear migration defects of *kar9* mutants (our unpublished results). Bim1p was tagged with the viral V5 epitope (Invitrogen) and expressed under the control of the *GAL1*-inducible promoter. As shown in Figure 2A, Kar9p::HA coimmunoprecipitated with Bim1p::V5, and the amount of Kar9p that coprecipitated was proportional to the amount of Bim1p that was expressed (compare lanes 3 and 4). As additional controls, immunoprecipitations were carried out in strains that did not contain the V5-tagged Bim1p plasmid (Figure 2A, lanes 1 and 2) or that contained a *KAR9* plasmid with no HA tag (Figure 2A, lanes 5 and 6). No HA-reactive bands were detected under these conditions.

In a reciprocal experiment, we first immunoprecipitated the Kar9p::HA with the use of anti-HA antibodies and probed the Western blot with V5 antibody to determine whether Bim1p coprecipitated. As seen in the bottom two panels of Figure 2A, Bim1p coimmunoprecipitated in the Bim1p-induced fraction (Figure 2A, lane 4) and was not detectable in the uninduced fraction (lane 3). However, a small fraction of Bim1p was found to pellet nonspecifically in the absence of Kar9p::HA (lane 6). This was also found to be independent of the presence of intact Kar9p and independent of the source of anti-HA antibodies (our unpublished results), indicating that some Bim1p may stick nonspecifically to the beads. Nevertheless, a significantly larger fraction of Bim1p was found in the fractions containing Kar9p::HA (compare lane 4 and lane 6). Together with the results from the initial V5 immunoprecipitation experiments, these results strongly argue that Bim1p specifically immunoprecipitates with Kar9p.

Interestingly, the HA immunoprecipitate contained two forms of Kar9p that differed by ~4000–5000 in apparent molecular weight (Figure 2, A and C). In contrast, only a single Kar9::HA form coprecipitated with Bim1p::V5. Electrophoresis on the same gel demonstrated that only the higher-molecular-weight form of Kar9p is complexed with Bim1p (our unpublished results). Although the molecular basis of the two forms of Kar9p is not yet known, the differential association with Bim1p suggests that there may be a significant functional or regulatory difference between them.

To confirm the *STU2–KAR9* interaction, we tested whether Kar9p could coimmunoprecipitate with HA epitope–tagged Stu2p. As shown in Figure 2B, wild-type Kar9p coimmunoprecipitated with Stu2p::HA (lane 2). In contrast, Kar9p was not found in the immunoprecipitates from strains lacking epitope-tagged Stu2p (lane 1) or in which no primary antibody was added to the extract (lane 5). Based on these data and the two-hybrid data, we conclude that Kar9p interacts with Stu2p.

We were unable to detect Stu2p in immunoprecipitates of epitope-tagged Kar9p. We believe that this is because the great majority of Kar9p is localized at the cell cortex, in complex with Bim1p and other proteins, whereas only a minor fraction of Kar9p is at the SPB in complex with Stu2p. Accordingly, the detection of the Stu2p in the Kar9p immunoprecipitates would require commensurably larger amounts of starting material and antibodies. It is also possible that placement of the epitope on Kar9p interferes with the interaction with Stu2p. Nevertheless, the localization of

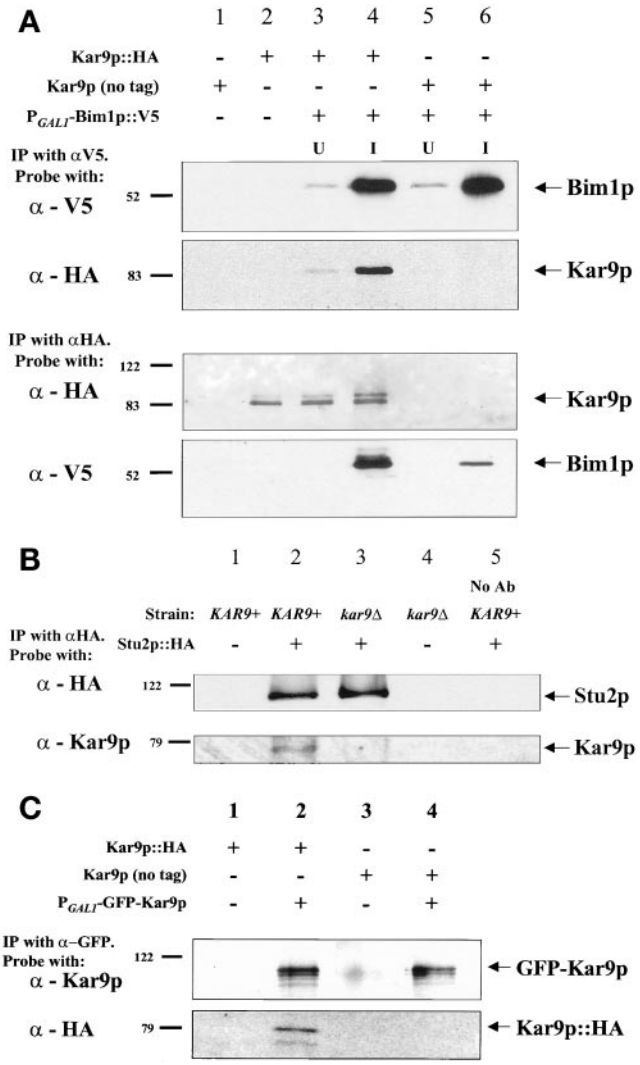

Figure 2. Kar9p coimmunoprecipitates with Bim1p, Stu2p, and Kar9p. (A) A *kar9*Δ stain (MS4263) containing HA epitope–tagged *KAR9* (pMR4723), nontagged *KAR9* (pMR4722), or galactose-inducible *BIM1*::V5 (pMR4620) plasmids were grown to mid exponential phase, and extracts were prepared for immunoprecipitation as described in MATERIALS AND METHODS. V5 antibody conjugated to Sepharose beads was used to immunoprecipitate Bim1p::V5. It was also used to probe Western blots. The HA antibody HA.11(16B12) conjugated to agarose beads was used to immunoprecipitate Kar9p::HA and probe the resulting Western blot. The HA antibody 12CA5 was used as a probe in the V5 immunoprecipitation experiment. Identical results were obtained when the two HA antibodies were used in any combination for either the immunoprecipitation step or subsequent Western blots. (B) Stu2p::HA was immunoprecipitated from extracts prepared from wild-type (MS1556) or *kar9*Δ (MS4306) strains containing HA epitope–tagged *STU2* (pWP70) or empty vector (pRS415; Sikorski and Hieter, 1989), as described in MATERIALS AND METHODS. Proteins from the precipitates were analyzed by Western blotting with the use of rabbit anti-Kar9p and the HA antibody 12CA5. (C) GFP–Kar9p was immunoprecipitated with the use of anti-GFP (a kind gift from Pamela Silver) from wild-type strains transformed with Kar9p:HA (pMR4723), Kar9p with no tag (pMR4722), and P_{GAL1}-GFP-Kar9p (pMR3464). Proteins from the precipitates were analyzed by Western blotting with the use of rabbit anti-Kar9p and the HA antibody 12CA5.

GFP–Kar9p (see below) further supports the validity of the interaction.

The two-hybrid screen also suggested that Kar9p self-associates. To test whether Kar9p physically associates with itself, GFP–Kar9p was induced in strains containing HA epitope–tagged Kar9p. Antibody against GFP was used to precipitate GFP–Kar9p and associated proteins. Western blots of the immunoprecipitates demonstrated that HA epitope–tagged Kar9p coprecipitated with GFP-Kar9p (Figure 2C, lane 2). Although the wild-type protein was also observed in the immunoprecipitates, it could not be unambiguously distinguished from proteolysis of the GFP–Kar9p (our unpublished results). In reciprocal experiments, the HA epitope–tagged form of Kar9p was immunoprecipitated first and GFP–Kar9p was found to coimmunoprecipitate with the use of Kar9p antibodies (our unpublished results). Based on these data and the two-hybrid data, we conclude that two or more molecules of Kar9p are present in the same complex and that Kar9p may self-associate.

Genetic Analysis Places Bim1p in the Kar9p Pathway for Nuclear Migration

Kar9p has been shown previously to function in a separate and partially redundant pathway for nuclear migration from the motor protein, cytoplasmic dynein (Miller and Rose, 1998). Deletion mutations in *KAR9* and *DHC1* are synthetically lethal with each other (Miller and Rose, 1998), whereas double mutants within the dynein pathway are viable and exhibit a phenotype no worse than either of the single mutants (Muhua *et al.*, 1994; Miller and Rose, 1998). Mutations in Bim1p/Yeb1p have been shown to be synthetically lethal with mutations in Arp1p/Act5p (Muhua *et al.*, 1998), a component of the dynactin complex that functions to activate dynein (Clark and Meyer, 1994). To determine whether Bim1p functions in the Kar9p pathway for nuclear migration, the *bim1*Δ mutant MS7310 was crossed to the *dhc1*Δ mutant MS4998. All of the 30 predicted double mutants failed to form viable colonies. We next crossed the *bim1*Δ mutant MS7310 to the *kar9*Δ mutant MS4315. Of 18 predicted double mutants, 15 were viable and exhibited no obvious growth defect compared with single mutants. Considering the two crosses together, the simplest interpretation is that Bim1p functions in the Kar9p branch of the nuclear migration pathway.

Mutations in BIM1 Eliminate Kar9p Localization along Microtubules but Do Not Affect Its Cortical or SPB Localization

Kar9p exhibits a cortical localization that is independent of microtubules (Miller and Rose, 1998). Because Bim1p is a microtubule-binding protein that localizes along nuclear and cytoplasmic microtubules (Schwartz *et al.*, 1997), we asked whether GFP–Kar9p's cortical localization was independent of this microtubule-associated protein. In 73% of *bim1*Δ cells, GFP–Kar9p was still localized at the tip of the bud (Figure 3). This demonstrated that Bim1p is not required for Kar9p's cortical localization.

In addition to Kar9p's localization to the cortical site, we have observed previously that some GFP–Kar9p also localizes along microtubules, displaying a linear or beaded appearance (Miller and Rose, 1998; Miller *et al.*, 1999). To test

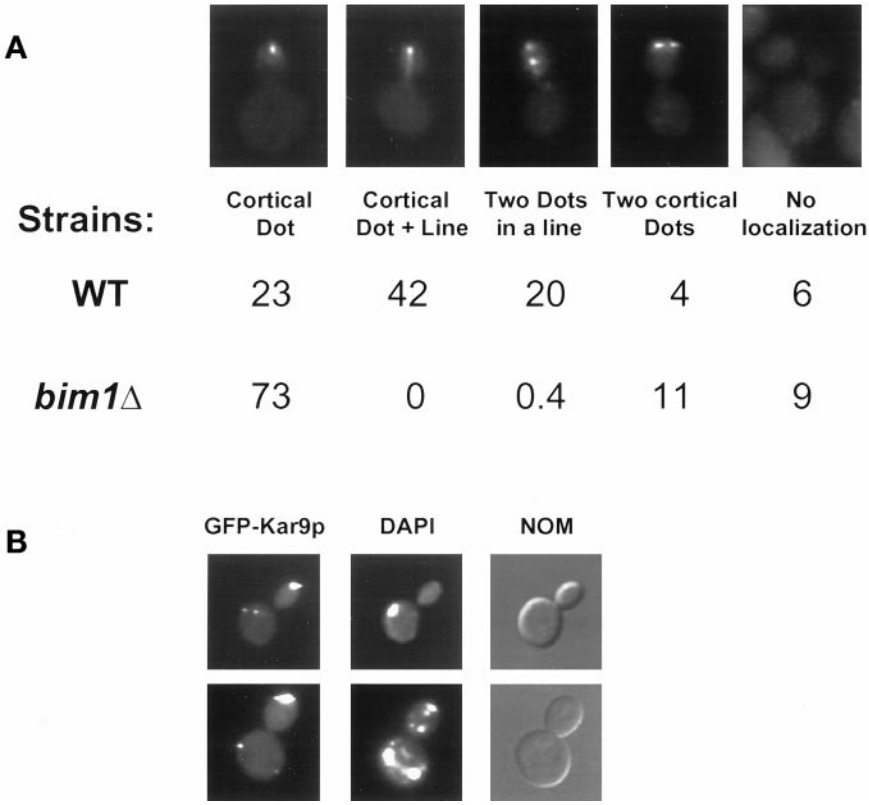

Figure 3. Bim1p is required for localization of GFP–Kar9p along microtubules but not for Kar9p localization at the SPB or cortex. (A) Wild-type (MS1556) and *bim1*Δ (MS7310) strains containing GFP–Kar9p (pMR3465) were grown to early exponential phase and induced for GFP-Kar9p expression. The percentage of cells exhibiting GFP-Kar9p expression in medium to large-budded cells with a single nucleus is shown under each representative cell (n = 720 for wild-type cells and 660 for *bim1*Δ cells). The average of three independent experiments is shown. Five percent of wild-type and 6% of *bim1*Δ cells exhibited GFP–Kar9p localization patterns that are not depicted. (B) A *bim1*Δ strain (MS7310) containing GFP–Kar9p (pMR3465) was grown and prepared as described in A.

whether GFP–Kar9p's localization along the length of the microtubules resulted from interaction with Bim1p, we scored Kar9p localization in *bim1*Δ cells. As shown in Figure 3, GFP–Kar9p's localization along cytoplasmic microtubules was completely dependent on Bim1p.

Among the cells with a cortical dot were some in which a second dot occurred closer to the nucleus. In previous reports, this class of cells was scored either as a separate category (see Figure 8 in Miller and Rose, 1998) or included in the "cortical dot" category (see Figure 10 in Miller and Rose, 1998). As shown in Figure 3, the "two dots in a line" category was completely dependent on the presence of Bim1p. Given the localization of Bim1p to microtubules, these data indicate that the proximally located dot is associated with microtubules, possibly at the end of a shorter microtubule bundle.

Upon closer examination of cells, we noticed a fainter dot of GFP–Kar9p fluorescence that was localized on the edge of the nucleus, as determined by staining of the DNA with the fluorescent dye DAPI. To investigate further, we scored whether cells with a dot at the tip of the bud also had one or two secondary dots on the nucleus. Eighty percent of *bim1*Δ cells and 84% of wild-type cells exhibited a pattern similar to that depicted in Figure 3B (top row), with one or two dots on the nucleus (n = 50 wild-type cells and 150 *bim*1Δ cells). The intensity of GFP fluorescence on the nucleus was always significantly less than the intensity of GFP–Kar9p fluorescence at the cortical site, as shown by the overexposure of the cortical spot (Figure 3B). The lower level of fluorescence intensity contributed to our previous characterization of the secondary dots as a minor localization pattern (Miller and Rose, 1998). The nuclear positioning defect of *bim1*Δ and the lack of microtubule-associated lines of GFP–Kar9p in the *bim1*Δ mutants also resulted in easier visualization of the nucleus-associated GFP–Kar9p fluorescence. In *bim1*Δ cells in which the nucleus had begun to divide aberrantly within the mother cell, two dots of GFP–Kar9p localization were observed that were always found at the distal ends of the bilobed nucleus (Figure 3B, bottom row). These observations suggest that Kar9p is associated with the SPB and that this localization is independent of Bim1p.

Bim1p Is Required for Efficient Cytoplasmic Microtubule Interaction with the Cortical GFP–Kar9p Dot

In large-budded cells, cytoplasmic microtubules intersect the cortical Kar9p dot (Miller and Rose, 1998). Given that Bim1p is localized along microtubules with a greater concentration at the tip of the cytoplasmic microtubule (Schwartz *et al.*, 1997; Tirnauer *et al.*, 1999), one model is that Bim1p would be at the ends of the cytoplasmic microtubule linking the microtubule to the Kar9p dot. If so, then the microtubules in *bim1*Δ mutants should not intersect the Kar9p dot. To determine whether Bim1p is required for the microtubule–Kar9p interaction, the orientation of cytoplasmic microtubules was examined in wild-type and *bim1*Δ cells by indirect immunofluorescence with tubulin and GFP antibodies. In 82% of wild-type large-budded cells with the nucleus positioned at the bud neck, the cytoplasmic bundle

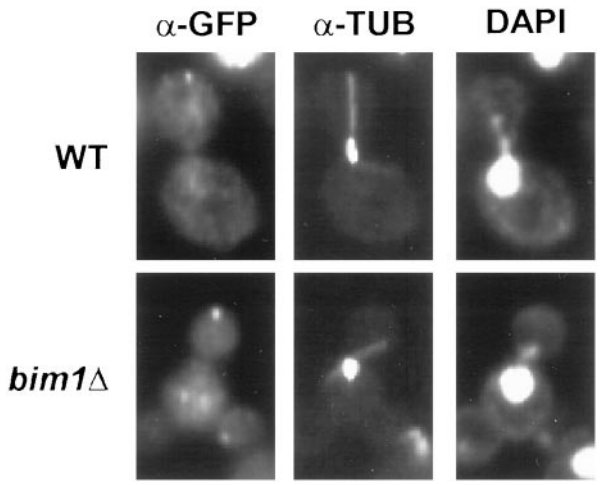

Figure 4. Cytoplasmic microtubules do not intersect the Kar9p dot in *bim1*Δ cells. Wild-type and *bim1*Δ cells containing GFP–Kar9p were fixed for double-label indirect immunofluorescence with the use of anti-GFP, anti-tubulin, and DAPI, as described in MATERIALS AND METHODS (n = 96 for wild-type cells and 105 for *bim1*Δ cells).

of microtubules intersected the GFP–Kar9p dot (Figure 4). In contrast, in only 11% of large-budded *bim1*Δ cells did the cytoplasmic bundle of microtubules intersect the GFP–Kar9p dot (Figure 4). Together, these data suggest that Bim1p plays a direct and major role in linking the cytoplasmic microtubules to the cortex at the Kar9p dot.

DISCUSSION

In yeast, spindle migration and orientation are dependent on the function of the cytoplasmic microtubules. In one popular model, cytoplasmic microtubules interact with the cell cortex to provide an anchor for forces acting on the microtubules. Potential forces acting on the microtubules include those generated by motor proteins (such as cytoplasmic dynein and the kinesin-related proteins Kip2 and Kip3) and by microtubule depolymerization. Regardless of the mechanism of force generation, a key component of the model is that the cortex would provide the necessary counterforce for movement. Strong experimental support for this model comes from Carminati and Stearns (1997), who showed that movement of the nucleus toward the bud is coordinated with interactions between the microtubules and the cortex.

A necessary component of spindle migration and orientation is a mechanism for designating the positional information for specifically targeting the nucleus to the bud. One model for targeting proposes that critical sites of productive microtubule–cortex interactions are restricted to a small region of the bud cortex. Consistent with this hypothesis, we have shown previously that Kar9p is required for microtubule orientation and localizes to a discrete cortical dot at the bud tip. The Kar9p dot is coincident with the end of a single microtubule (or bundle of microtubules) that is observed by fixation and immunofluorescence. Nevertheless, it has remained unclear whether Kar9p's interacts directly with the microtubule or indirectly through a microtubule-associated protein.

In this report, we present evidence that the cytoplasmic microtubule(s) interact with the cortical Kar9p protein via the microtubule-associated protein Bim1p/Yeb1p. First, Kar9p was found to associate with Bim1p/Yeb1p by both two-hybrid screening and reciprocal coimmunoprecipitation criteria. Second, Kar9p localization along the length of the cytoplasmic microtubules, but not to the cortical dot, was dependent on Bim1p. Third, by genetic criteria, Bim1p was found to function most likely in the Kar9p/Kip3p pathway for nuclear migration. Finally, the interaction of the cytoplasmic microtubules with the Kar9p cortical dot was found to be dependent on Bim1p.

The minimal region of Bim1p/Yeb1p interaction with Kar9p that we defined encompasses an 89-amino acid region in the third quarter of Bim1p. This region includes two highly conserved motifs found in all EB1 homologues, including those from vertebrates, invertebrates, and fungi (Figure 2, D and E). Furthermore, the second motif, including the sequence ILYAT, was found to be required for the two-hybrid interaction. Although the first motif was not tested directly, the distribution of plasmids obtained from the two-hybrid screen strongly suggests that this region is also required. Further delineation of the region will require specific mutations in this interval.

The conservation of the Kar9p interaction region in EB1 proteins strongly suggests that interaction with a Kar9p-like protein has been critical for the function of EB1-related proteins throughout evolution. Although Kar9p homologues have not yet been identified in other organisms, the specific region of Kar9p that interacts with EB1 may be small and/or degenerate and therefore is difficult to find by homology-based searching algorithms. Regardless, the known functions of EB1 suggest that it may play a general role in coordinating cell polarization and microtubule orientation. The human EB1 protein is a binding partner for APC, a protein mutated in a majority of familial colon cancers (Ichii *et al.*, 1993; Levy *et al.*, 1994), and both proteins interact with the ends of microtubules. APC normally plays a role in the Wnt/β-catenin signaling pathway, which is important in establishing embryonic polarity and pattern formation in a number of systems (Barker *et al.*, 2000). Thus, EB1 and Bim1p may both play related roles in recognizing the inherent cellular polarity and translating that into positional information that is used for signaling and spindle positioning. In the case of yeast, Bim1p and Kar9p couple microtubule orientation to actin-based cell polarity signals via the formin homologue Bni1p. In the case of vertebrate cells, the coupling appears to be between the microtubules and the catenin-containing focal adhesions (Kaverina *et al.*, 1998).

The observation that both Bim1p and Kar9p localize along the sides of the microtubules is intriguing given their implied role in "microtubule capture." A simple model in which the microtubules are bound via their exposed plus ends would not predict this behavior. Instead, it argues that capture is via the interactions along the sides of the microtubules, perhaps to form a sliding collar-like attachment. Similar sliding collars have been hypothesized to be important in kinetochore-dependent chromosome movement. In both cases, a sliding collar would allow stable attachment to the end of a microtubule, which is otherwise undergoing

shortening from its plus end. Recent data from Maddox *et al.* (1999, 2000) have demonstrated such shortening from the plus ends of the cytoplasmic microtubules during nuclear migration in yeast cells.

Given the possibility of association along the sides of the microtubules, it is striking that in most cases in which Kar9p is seen to localize along the length of the microtubules it is always brightest at the distal (cortical) end. What limits its localization so that it is not found more proximally? Although it is possible that the tubulin at the distal ends is qualitatively different (e.g., still contained GTP rather than GDP), we favor a model in which the localization of Kar9p is restricted by its interaction with Bni1p at the cortex. One argument in favor of this model is that within 10 min after depolymerization of actin in shmoos by latrunculin A, Kar9p is found uniformly localized along the cytoplasmic microtubules. We hypothesize that Kar9p interacts with both Bni1p and Bim1p at the distal end of the microtubules but only with Bim1p along the sides. This model further assumes that either Kar9p or Bim1p (or both) self-associates to cluster the localization. From this perspective, it is intriguing that we also identified Kar9p in the two-hybrid screen, strongly suggesting that Kar9p interacts with itself. The basic carboxyl-terminal region of Kar9p was not required for the interaction, implicating the central and/or amino-terminal domains as being required for the interaction. Consistent with this observation, the central region of Kar9p contains two regions, each ~30 residues long, which are strongly predicted to form coiled coils (Lupas *et al.*, 1991; Miller and Rose, 1998). Self-association of Kar9p may help the protein to localize to discrete sites within the cell instead of to a more diffuse localization.

Although our experiments used GFP–Kar9p expressed under the control of *GAL1*, the association of GFP–Kar9p was also seen in concurrent experiments with the same GFP–Kar9p construct under the control of the *KAR9* promoter (Lee *et al.*, 2000). Therefore, it is highly unlikely that the association of Kar9p along the sides of the microtubules reflects the effects of overexpression.

Bim1p has been reported to play a significant role in regulating microtubule dynamics, such that the *bim1*Δ mutant contains shorter but less dynamic cytoplasmic microtubules during G1 (Tirnauer *et al.*, 1999). This observation suggests a regulatory model for the interaction between Kar9p and Bim1p, such that Kar9p would regulate Bim1p's effects on microtubule dynamics. Bim1p, free of Kar9p, would destabilize microtubules; interaction with the cortical Kar9p would then cause Bim1p to stabilize the microtubules. The microtubule would thereby become transiently anchored to the cortex, where other proteins such as the kinesin-related protein Kip3p would then facilitate shortening. Consistent with this model is the striking difference between time-lapse observations of microtubules in live cells and the appearance of the microtubules in fixed cells. Live-cell images usually show multiple dynamic cytoplasmic microtubules (Carminati and Stearns, 1997), whereas fixed preparations usually show a single microtubule bundle that is often associated with the cortex. Presumably, the cortically anchored microtubules are more stable and thereby uniquely preserved during fixation.

The shorter cytoplasmic microtubules in the *bim1* mutant raises the question of whether the cytoplasmic microtubules are misoriented because they are simply too short to interact with the cortical Kar9p. We believe that this is unlikely for several reasons. First, consider the behavior of other mutants that also lead to shorter cytoplasmic microtubules. Both *bik1* and *kip2* mutants exhibit shorter microtubules, yet genetic tests demonstrated that each mutant remains dependent on the activity of Kar9p for nuclear migration and viability. This is quite unlike the behavior of *bim1* mutants, in which Kar9p is dispensable for life. Furthermore, at least in the case of the *kip2* mutant, the Kar9p dot localized near the SPB/bud neck (Miller *et al.*, 1998), as if the position of the Kar9p dot is determined by a dynamic balance between the cortical and microtubule interactions. Second, some of the large-budded cells contained cytoplasmic microtubules that would have been long enough to contact the cortex (i.e., similar to the length of the long axis of the bud), yet this was insufficient to contact the Kar9p dot. This observation has been confirmed by concurrent studies from the Pellman laboratory (Lee *et al.*, 2000). Finally, while this article was under review, two papers appeared that reported the direct interaction of Kar9p with Bim1p. Copelleting assays in vitro were used, and both papers reported that Kar9p interacts with microtubules in a Bim1p-dependent manner (Korinek *et al.*, 2000; Lee *et al.*, 2000), confirming the in vivo data.

In this study, we found that a large percentage of budded cells also displayed a fainter Kar9p localization at or near the SPB. This observation is consistent with previous findings that Kar9p seemed to have a secondary localization at the SPB, which was often prominent in mutants that affected its cortical localization or when Kar9p was overexpressed. At the same time, we isolated *STU2* in the two-hybrid screen and showed that the two proteins coimmunoprecipitate. An interaction between Kar9p and Stu2p, a component of the SPB, would explain the putative SPB localization of Kar9p. Interestingly, Stu2p also has been found to interact with Bim1p by two-hybrid analysis (Wang and Huffaker, 1997). However, we demonstrated that Bim1p is not required for Stu2p's two-hybrid interaction with Kar9p (Figure 1B), eliminating the possibility that Kar9p and Stu2p interact only through a ternary complex containing Bim1p. Furthermore, Bim1p was not required for Kar9p localization near the SPB (Figure 3B).

Stu2p also binds to the sides of microtubules. The microtubule-binding domain of Stu2p lies within residues 558–658 (Wang and Huffaker, 1997). Within the domain are two repeats of a smaller motif. The smallest of the four Stu2p two-hybrid fusions that interacts with Kar9p begins at residue 649 and contains only 9 residues from one of the microtubule-binding motifs. This represents less than a quarter of a binding motif. Wang and Huffaker (1997) demonstrated that half of one binding motif is not sufficient to confer microtubule binding in vitro. Therefore, it is highly unlikely that the microtubule-binding domain mediates Stu2p's interaction with Kar9p.

The biological significance of Kar9p localization to the vicinity of the SPB is uncertain. It is worth noting that Bim1p has been implicated as mediating a cytokinesis checkpoint, such that cytokinesis is not initiated until anaphase has been successfully completed and the bud has received a nucleus (Muhua *et al.*, 1998). The mechanism by which the cell could determine that a nucleus is in the bud is unclear. It is tempting to speculate that the interaction between Bim1p,

Kar9p, and Stu2p may be part of the mechanism. We propose that Kar9p is localized normally only to the bud tip cortex, where it can interact with Bim1p on the microtubules. As a result of spindle elongation, the SPB is driven into the bud, where it comes close to the bud cortex. The close proximity of the SPB with the bud cortex then allows Stu2p to interact with Kar9p, perhaps displacing Bim1p from Kar9p, whereupon a signal is sent that the SPB has entered the bud and elongation is complete. In support of this hypothesis, the *bni1 kar9* double mutant was observed to have an increased frequency of anucleate cells relative to either single mutant (Miller *et al.*, 1999), consistent with a possible role for Kar9p in the checkpoint control.

The finding of two different molecular weight species of Kar9p supports the possibility of different functions for Kar9p. Although at present we do not understand the molecular basis for the different forms, only the higher-molecular-weight form interacts with Bim1p. The different forms may reflect regulation of Kar9p's interaction with Bim1p, Stu2p, or the Bni1p complex. We believe that the lower form is not an artifact of proteolytic degradation in vitro because Kar9p was relatively resistant to proteolysis under conditions in which Bim1p was clearly degraded (our unpublished observations).

In summary, in this paper we identify Bim1p as a critical microtubule-associated protein that interacts with Kar9p to link the nucleus to the cell cortex. The linkage allows cortical actin–based cell polarization information to be translated into a form that can be used to direct the microtubule-based nuclear migration. Given the strong conservation of formins and EB1 homologues, it will be interesting to determine whether there are other Kar9p homologues that couple the actin and microtubule cytoskeletons.

ACKNOWLEDGMENTS

The authors thank Naz Erdeniz and Eugenia Xu for helpful comments. This work was supported by grant GM37739 from the National Institutes of Health.

REFERENCES

Barker, N., Morin, P.J., and Clevers, H. (2000). The yin-yang of TCF/beta-catenin signaling. Adv. Cancer Res. *77*, 1–24.

Barth, A.I., Nathke, I.S., and Nelson, W.J. (1997). Cadherins, catenins and APC protein: interplay between cytoskeletal complexes and signaling pathways. Curr. Opin. Cell Biol. *9*, 683–690.

Berlin, V., Styles, C.A., and Fink, G.R. (1990). *BIK1*, a protein required for microtubule function during mating and mitosis in *Saccharomyces cerevisiae*, colocalizes with tubulin. J. Cell Biol. *111*, 2573–2586.

Berrueta, L., Kraeft, S.K., Tirnauer, J.S., Schuyler, S.C., Chen, L.B., Hill, D.E., Pellman, D., and Bierer, B.E. (1998). The adenomatous polyposis coli-binding protein EB1 is associated with cytoplasmic and spindle microtubules. Proc. Natl. Acad. Sci. USA *95*, 10596–10601.

Byers, B. (1981). Cytology of the yeast life cycle. In: The Molecular Biology of the Yeast *Saccharomyces*: Life Cycle and Inheritance, ed. J. Strathern, E.W. Jones, and J.R. Broach, Cold Spring Harbor, NY: Cold Spring Harbor Laboratory, 59–96.

Carminati, J.L., and Stearns, T. (1997). Microtubules orient the mitotic spindle in yeast through dynein-dependent interactions with the cell cortex. J. Cell Biol. *138*, 629–641.

Chen, X.P., Yin, H., and Huffaker, T.C. (1998). The yeast spindle pole body component Spc72p interacts with Stu2p and is required for proper microtubule assembly. J. Cell Biol. *141*, 1169–1179.

Clark, S.W., and Meyer, D.I. (1994). *ACT3*: a putative centractin homologue in *S. cerevisiae*, is required for proper orientation of the mitotic spindle. J. Cell Biol. *127*, 129–138.

Cottingham, F.R., and Hoyt, M.A. (1997). Mitotic spindle positioning in *Saccharomyces cerevisiae* is accomplished by antagonistically acting microtubule motor proteins. J. Cell Biol. *138*, 1041–1053.

DeZwaan, T.M., Ellington, E., Pellman, D., and Roof, D.M. (1997). Kinesin-related *KIP3* of *Saccharomyces cerevisiae* is required for a distinct step in nuclear migration. J. Cell Biol. *138*, 1023–1040.

Farkasovsky, M., and Kuntzel, H. (1995). Yeast Num1p associates with the mother cell cortex during S/G2 phase and affects microtubular functions. J. Cell Biol. *131*, 1003–1014.

Gietz, R.D., and Schiestl, R.H. (1995). Transforming yeast with DNA. Methods Mol Cell. Biol. *5*, 255–269.

Groden, J., *et al.* (1991). Identification and characterization of the familial adenomatous polyposis coli gene. Cell *66*, 589–600.

Harlow, E., and Lane, D. (1988). Antibodies: A Laboratory Manual, Cold Spring Harbor, NY: Cold Spring Harbor Laboratory.

Hoffman, D.S., and Winston, F. (1987). A ten minute DNA preparation from yeast efficiently releases autonomous plasmids for transformation of *E. coli*. Gene *57*, 267–272.

Ichii, S., *et al.* (1993). Detailed analysis of genetic alterations in colorectal tumors from patients with and without familial adenomatous polyposis (FAP). Oncogene *8*, 2399–2405.

James, P., Halladay, J., and Craig, E.A. (1996). Genomic libraries and a host strain designed for highly efficient two-hybrid selection in yeast. Genetics *144*, 1425–1436.

Kahana, J.A., Schlenstedt, G., Evanchuk, D.M., Geiser, J.R., Hoyt, M.A., and Silver, P.A. (1998). The yeast dynactin complex is involved in partitioning the mitotic spindle between mother and daughter cells during anaphase B. Mol. Biol. Cell *9*, 1741–1756.

Kaverina, I., Rottner, K., and Small, J.V. (1998). Targeting, capture, and stabilization of microtubules at early focal adhesions. J. Cell Biol. *142*, 181–190.

Korinek, W.S., Copeland, M.J., Chaudhuri, A., and Chant, J. (2000). Molecular linkage underlying microtubule orientation toward cortical sites in yeast. Science *287*, 2257–2259.

Lee, L., Klee, S.K., Evangelista, M., Boone, C., and Pellman, D. (1999). Control of mitotic spindle position by the *Saccharomyces cerevisiae* formin Bni1p. J. Cell Biol. *144*, 947–961.

Lee, L., Tirnauer, J.S., Li, J., Schuyler, S.C., Liu, J.Y., and Pellman, D. (2000). Positioning of the mitotic spindle by a cortical-microtubule capture mechanism. Science *287*, 2260–2262.

Levy, D.B., Smith, K.J., Beazer-Barclay, Y., Hamilton, S.R., Vogelstein, B., and Kinzler, K.W. (1994). Inactivation of both APC alleles in human and mouse tumors. Cancer Res. *54*, 5953–5958.

Lupas, A., Van Dyke, M., and Stock, J. (1991). Predicting coiled coils from protein sequences. Science *252*, 1162–1164.

Maddox, P., Chin, E., Mallavarapu, A., Yeh, E., Salmon, E.D., and Bloom, K. (1999). Microtubule dynamics from mating through the first zygotic division in the budding yeast *Saccharomyces cerevisiae*. J. Cell Biol. *144*, 977–987.

Maddox, P.S., Bloom, K.S., and Salmon, E.D. (2000). The polarity and dynamics of microtubule assembly in the budding yeast *Saccharomyces cerevisiae*. Nat. Cell Biol. *2*, 36–41.

McMillan, J.N., and Tatchell, K. (1994). The *JNM1* gene in the yeast *Saccharomyces cerevisiae* is required for nuclear migration and spindle orientation during the mitotic cell cycle. J. Cell Biol. *125*, 143–158.

Miller, R.K., Heller, K.K., Frisen, L., Wallack, D.L., Loayza, D., Gammie, A.E., and Rose, M.D. (1998). The kinesin-related proteins, Kip2p and Kip3p, function differently in nuclear migration in yeast. Mol. Biol. Cell *9*, 2051–2068.

Miller, R.K., Matheos, D., and Rose, M.D. (1999). The cortical localization of the microtubule orientation protein, Kar9p, is dependent upon actin and proteins required for polarization. J. Cell Biol. *144*, 963–975.

Miller, R.K., and Rose, M.D. (1998). Kar9p is a novel cortical protein required for cytoplasmic microtubule orientation in yeast. J. Cell Biol. *140*, 377–390.

Morrison, E.E., Wardleworth, B.N., Askham, J.M., Markham, A.F., and Meredith, D.M. (1998). EB1, a protein which interacts with the APC tumor suppressor, is associated with the microtubule cytoskeleton throughout the cell cycle. Oncogene *17*, 3471–3477.

Muhua, L., Adames, N.R., Murphy, M.D., Shields, C.R., and Cooper, J.A. (1998). A cytokinesis checkpoint requiring the yeast homologue of an APC-binding protein. Nature *393*, 487–491.

Muhua, L., Karpova, T.S., and Cooper, J.A. (1994). A yeast actin-related protein homologous to that in vertebrate dynactin complex is important for spindle orientation and nuclear migration. Cell *78*, 669–679.

Palmer, R.E., Sullivan, S.D., Huffaker, T., and Koshland, D. (1992). Role of astral microtubules and actin in spindle orientation and migration in the budding yeast, *Saccharomyces cerevisiae*. J. Cell Biol. *119*, 583–593.

Rose, M.D., Winston, F., and Hieter, P. (1990). Methods of Yeast Genetics, Cold Spring Harbor, NY: Cold Spring Harbor Laboratory.

Rothstein, R.J. (1983). One-step gene disruption in yeast. Methods Enzymol. *101*, 202–211.

Saunders, W., Hornack, D., Lengyel, V., and Deng, C. (1997). The *Saccharomyces cerevisiae* kinesin-related motor Kar3p acts at preanaphase spindle poles to limit the number and length of cytoplasmic microtubules. J. Cell Biol. *137*, 417–431.

Schwartz, K., Richards, K., and Botstein, D. (1997). *BIM1* encodes a microtubule-binding protein in yeast. Mol. Biol. Cell *8*, 2677–2691.

Shaw, S.L., Yeh, E., Maddox, P., Salmon, E.D., and Bloom, K. (1997). Astral microtubule dynamics in yeast: a microtubule-based searching mechanism for spindle orientation and nuclear migration into the bud. J. Cell Biol. *139*, 985–994.

Sikorski, R.S., and Hieter, P. (1989). A system of shuttle vectors and yeast host strains designed for efficient manipulation of DNA in *Saccharomyces cerevisiae*. Genetics *122*, 19–27.

Su, L.K., Burrell, M., Hill, D.E., Gyuris, J., Brent, R., Wiltshire, R., Trent, J., Vogelstein, B., and Kinzler, K.W. (1995). APC binds to the novel protein EB1. Cancer Res. *55*, 2972–2977.

Sullivan, D.S., and Huffaker, T.C. (1992). Astral microtubules are not required for anaphase B in *Saccharomyces cerevisiae*. J. Cell Biol. *119*, 379–388.

Theesfeld, C.L., Irazoqui, J.E., Bloom, K., and Lew, D.J. (1999). The role of actin in spindle orientation changes during the *Saccharomyces cerevisiae* cell cycle. J. Cell Biol. *146*, 1019–1032.

Tirnauer, J.S., O'Toole, E., Berrueta, L., Bierer, B.E., and Pellman, D. (1999). Yeast Bim1p promotes the G1-specific dynamics of microtubules. J. Cell Biol. *145*, 993–1007.

Trueheart, J., Boeke, J.D., and Fink, G.R. (1987). Two genes required for cell fusion during yeast conjugation: evidence for a pheromone-induced surface protein. Mol. Cell. Biol. *7*, 2316–2328.

Wach, A., Brachat, A., Pohlmann, R., and Philippsen, P. (1994). New heterologous modules for classical or PCR-based gene disruptions in *Saccharomyces cerevisiae*. Yeast *10*, 1793–1808.

Wang, P.J., and Huffaker, T.C. (1997). Stu2p: a microtubule-binding protein that is an essential component of the yeast spindle pole body. J. Cell Biol. *139*, 1271–1280.

Yeh, E., Skibbens, R.V., Cheng, J.W., Salmon, E.D., and Bloom, K. (1995). Spindle dynamics and cell cycle regulation of dynein in the budding yeast, *Saccharomyces cerevisiae*. J. Cell Biol. *130*, 687–700.